Master of Science Thesis in Electrical Engineering
Department of Electrical Engineering, Linköping University, 2018

Control Oriented Modeling of Engine Out Temperatures

Lars Malm

LINKÖPING UNIVERSITY

Master of Science Thesis in Electrical Engineering

Control Oriented Modeling of Engine Out Temperatures

Lars Malm

LiTH-ISY-EX--18/5156--SE

Supervisor: **Xavier LIamas Comellas**
ISY, Linköping university
Andreas Thomasson
ISY, Linköping university
Martin Larsson
Volvo Car Corporation

Examiner: **Professor Lars Eriksson**
ISY, Linköping university

Vehicular Systems
Department of Electrical Engineering
Linköping University
SE-581 83 Linköping, Sweden

Abstract

To have knowledge about the exhaust temperature is of great importance in several ways. Knowing the exhaust temperature means that it is easier to protect the catalyst and turbine from too high temperatures but it also important in controlling the turbine power.
In this thesis a physically based model of the engine out temperature is developed. The model is built up by two different cylinder pressure models and one engine out temperature model. Measurements has been made using a test engine at Linköping University. These measurement has then been used to parameterize and validate the model.
Since the measurements of the engine out port temperature are not showing reasonable temperatures, the temperatures in the pipes has been used for validation. That makes the results less reliable since no heat transfer between the port and pipe are considered in the model.

Acknowledgments

I would like to thank Volvo Cars for giving me the opportunity to write this thesis, specially my supervisor Martin Larsson for all the help and guidance during the project. I also want to thank my supervisors at Linköping University, Andreas Thomasson and Xavier Llamas Comellas, who assisted me with advice when writing this thesis. I also would like to thank research engineer Tobias Lindell for all the help in the test lab. Finally I would like to thank my examiner Professor Lars Eriksson for making this thesis a reality and for all his work that has been important for this thesis.

Linköping, June 2018
Lars Malm

Contents

Notation

Abbreviations

Abbreviation	Description
IVO	Intake Valve Opening
EVO	Exhaust Valve Opening
IVC	Intake Valve Closing
EVC	Exhaust Valve Closing
EXH	End of Blow Down
INT	Start of Intake Valve Closing
TDC	Top Dead Center
BTDC	Before Top Dead Center
ATDC	After Top Dead Center
BDC	Bottom Dead Center
CAD	Crank Angle Degree
MFB	Mass Fraction Burned

1 Introduction

For developing and calibration of engine control systems the exhaust temperature is significant. Too high exhaust temperatures could cause damage in the turbine and the catalyst and therefore the ability to estimate the exhaust temperature is of high importance. In today's exhaust systems no temperatures are measured by sensors. Instead the temperatures are estimated by using map-based models. However, due to stricter diagnostic requirements the accuracy of these models has been questioned. Therefore, new models with higher accuracy are sought after.

1.1 Problem Formulation

High exhaust temperatures can cause extensive damage to the turbocharger and the catalyst. Therefore it is of high importance that good estimates of the exhaust temperature are available, to be used for protection, control and diagnostic purposes. Nowadays temperature estimations are map-based which are not accurate enough and are hard to calibrate. Physically based models are easier to calibrate since they are based on physics, less measurement points should therefore be required to tune and adjust the models.
This thesis work aims at developing physically based temperature models which capture the influence of different control signals. Furthermore, the models should be of low computational complexity, so that they can be implemented in the control system. The ultimate goal of this exhaust temperature model is to give more accurate predictions to enable better control and diagnostic performance and replace the current map-based models.

1.2 Purpose and Goal

The purpose is to build a physically based model of the exhaust temperature. The model should be used to improve the engine control system, with the principal objective of protecting vulnerable components from overheating. The proposed model should capture the effects of:

- Different ignition angles
- Variations in air/fuel-ratio
- Variations in intake temperature, engine speed, intake pressure, exhaust back pressure, etc.

1.3 Expected results

The model will be developed using measurement data from the test engine at Linköping university. The developed models will then be validated with some other reserved data. Test data will be obtained by driving the engine in different operation points with different ignition timings and air/fuel-ratios. Analytical calculations of cylinder pressures and exhaust temperatures should be validated against measured data from the test engine. The end-criteria of the project is to develop a model that is sufficiently accurate to the gathered data. Since the aim of the models is to minimize the relative errors between measured values and modeled values, plots that show the relative errors are going to be presented for each sub model.

1.4 Outline

The structure of the report can be seen below. The report consists of five chapters.

- **Introduction**
  In the introduction chapter the problem formulation, expected results, purpose and goals are discussed.
- **Related Research**
  A related research that contains the state of the art in exhaust temperature modeling is then presented.
- **Measurements**
  The measurement chapter explains the measurement process, sensor placement etc.
- **Modeling**
  This chapter treats the modeling process, including theory and all details about the used models.

- **Results**
  The results are then presented and the model is validated with measurement data.
- **Discussion**
  The results from the previous chapter are discussed here.
- **Conclusions**
  Finally, the last chapter of the thesis contains conclusions and some thoughts about future work.

2

Related Research

2.1 State of the Art

For modeling the exhaust temperature it is of great importance to get a good estimate of the intake pressure and temperature in the cylinder before the engine cycle starts. To know the temperature T_{IVC} (temperature at intake valve closing) the fraction of residual gases needs to be estimated.
In Ainouz and Vedholm [1], the authors estimate the residual gas fraction and the temperature at intake valve closing by an iteration method based on nominal assumptions of the Otto cycle. This method utilizes the ideal gas law. In Eriksson and Nielsen [9] a fixed point iteration is used to estimate T_{IVC}, x_r and T_r. A similar method is described in Mladek and Onder [20] where an analysis of the in-cylinder temperature is performed. A complete dynamic intake and exhaust flow simulation for spark ignition IC engines has been developed in Meisner and Sorenson [19]. The model neglects frictional effects but still accurately models the temperature transients of the exhaust gases. A description of the engine heat transfer for the investigation of global thermal behaviour has been provived in Shayler et al. [25]. A model of in-cylinder air mass and residual gas fraction of a turbocharged SI engine with Variable Valve Timing (VVT) actuators is developed in Leroy et al. [16]. Even if the model could not be compared with any measurements, there was shown that a limited experimental data set is sufficient to calibrate the model. Residual gas models are evaluated and validated in Fox et al. [11], Ponti et al. [22] and Öberg and Eriksson [21]. Fox et al. [11] captures the impact from different values of intake pressure, engine speed, and valve overlap timings whilst Ponti et al. [22] also involves EGR. In Öberg and Eriksson [21] models are built for a variable cam timing engine (VCT). Another residual gas fraction estimation is made in Cavina et al. [4]. This model is based on Senecal et al. [24] and Fox et al. [11], but has been extended to take into account also the

presence of externally recirculated exhaust gas (external EGR), and also highlight the effects of different valve timings.

An analytic model of the pressure and temperature during the compression and expansion phase is derived and validated in Eriksson and Andersson [8]. The pressure model is given in closed form and there is no need to numerically solve any ordinary differential equations. This low computationally demanding approach is thus suitable to be implemented in engine control units (ECUs). The model assumes polytropic processes during both compression and expansion and can capture variations in ignition timing and air/fuel-ratio with good accuracy. Since the exhaust temperature is highly dependent on the cylinder pressure, this paper contains valuable information that can be used in this thesis. In Hashemzadeh Nayeri [14], similar work is made where an analysis of the in-cylinder temperature is performed. Unfortunately, this model has not been validated due to absence of validation data. Gas leaks between cylinder and piston are named crevice effects and have been taken into consideration for crank angle based cylinder pressure models in Smith [26]. In Draper [5], the author shows that the pressure waves appearing in the cylinder can be described with the physical laws of sound waves.

Regarding temperature modeling, several works are published in the literature. An affine model for the temperature at the exhaust valve as a function of the mass flow is developed in Eriksson [7]. This paper shows that, for a spark ignited engine operating at MBT and stoichiometric conditions, it is sufficient to model the engine out temperature as a linear function of mass flow. In Ericson et al. [6], it is shown that both exhaust gas recirculation and water injection can decrease the exhaust temperature. In Tesfa et al. [27], it is shown that there are not any significant differences on the peak cylinder pressure and the heat release rate of CI engine running with biodiesel when injecting water in the intake manifold.

To develop an exhaust temperature model, it is important to take heat transfers into consideration. In Caton and Heywood [3] models were developed for the instantaneous heat transfer, fluid mixing, and hydrocarbon oxidation in an engine exhaust port. This could be included in the physical model that this thesis aims to develop. A heat release analysis procedure that maintains simplicity while including the effects of heat transfer, crevice flows and fuel injection is developed and tested in Gatowski et al. [13]. This method needs a crank angle based cylinder pressure model which means the model needs to solve differential equations. An experimental analysis of the heat transfer in the combustion chamber of an air-cooled diesel engine is carried out in Mavropoulos et al. [18], which reveals significant differences between the overall and local peak heat transfer coefficient values in the cylinder head surface. A diesel engine is also handled in Jennings and Morel [15], where the wall temperature effects on the engine heat transfer are studied. Models of the heat transfer between gas and cylinder walls in a two-stroke engine are developed in Franco and Martorano [12], where the

authors shows that temperature is not uniform in the radial direction.

A method for using UEGO-sensors (modern universal exhaust gas oxygen) to measure exhaust gas temperature is proposed and analyzed in Martin and Rocci [17]. The authors shows that this method can provide an accurate measurement of exhaust gas temperature in dynamic drive conditions. An absorption-based diode laser sensor for temperature measuring has been validated in Rieker et al. [23]. The paper contains crank angle-resolved measurements of gas temperature during the compression stroke of an internal combustion. The sensor was applied to two different internal combustion engines and it was shown that the sensor is accurate.

3

Measurements

Measurements was done by using the test engine at the division of vehicular systems, Linköping university. The purpose of the measurements was to provide data that could be used to validate the model. An exhaust manifold with variously placed sensors was provided from VCC and then installed on the test engine.

3.1 Operating points

The tests was performed at 3 different speeds and 3 different loads. The idea about the operating points was to get data from a varying range of speeds and loads.

The chosen speeds and loads was

- N - 1500, 3000, 4500 rpm
- Tq - 50, 150, 300 Nm

which resulted in 9 operating points.

3.2 Sensor placement

The exhaust manifold that was used in the measurements is a dual wall manifold. The first layer consists of four pipes from each cylinder that all connects in a small volume before the turbocharger. Secondly, there is a metallic layer that covers all four pipes. Three different temperature sensors was used for the measurements, one unexposed thermocouple, one exposed thermocouple and one fine wire thermocouple. The unexposed thermocouple has a longer response time and need more time to stabilize due a protecting and isolating mantle around it. On the

exposed thermocouple there is no mantle which makes it a bit faster. The fine wire thermocouple is by far the most responsive temperature sensor but is also very sensitive. For that reason, the fine wire thermocouple can not be used in all operating points to keep it away from too high temperatures.

The placement of the sensors can be seen in Figure 3.1. A description of all sensors follows below

1. Port gas temperature - Cylinder 1 - Unexposed thermocouple
2. Port gas temperature - Cylinder 2 - Unexposed thermocouple
3. Port gas temperature - Cylinder 3 - Exposed thermocouple
4. Port gas temperature - Cylinder 4 - Exposed thermocouple
5. Port surface temperature - cylinder 1
6. Port surface temperature - cylinder 2
7. Port surface temperature - cylinder 3
8. Port surface temperature - cylinder 4
9. Pipe gas temperature - cylinder 3 - Exposed thermocouple
10. Pipe gas temperature - cylinder 4 - Exposed thermocouple
11. Gas temperature collector - Exposed thermocouple
12. Pressure collector

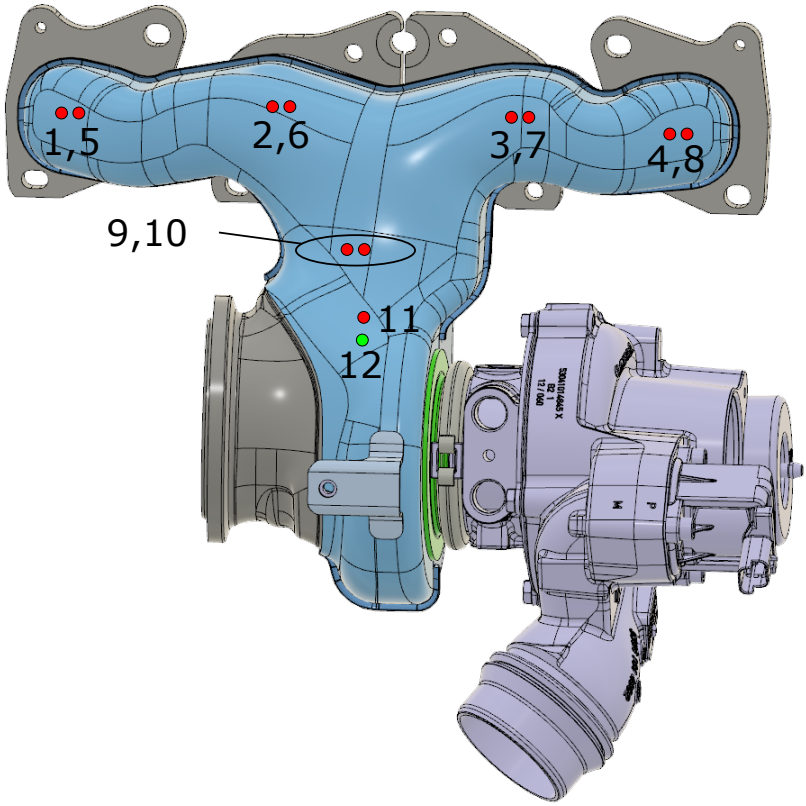

Figure 3.1

Other measured data that is needed for the model is

- Cylinder pressure
- Intake manifold pressure

Since the model should capture variations in λ and ignition timing, these variations should be included in the measurements. Table 3.1 shows in which points these measurements are performed.

Table 3.1: *An overview of the measuring operating points.*

	50 Nm	**150 Nm**	**300 Nm**
1500rpm	Stationary meas.	Stationary meas.+λ+θ_{ign}	Stationary meas.
3000rpm	Stationary meas.	Stationary meas.	Stationary meas.
4500rpm	Stationary meas.	Stationary meas.	Stationary meas.

When doing the measurements the intake air was set to a constant value. Before the sampling was done, the engine was running at the current operating point for 3-4 minutes so the temperature sensors had enough time to stabilize.

3.3 Variations in lambda - λ

Variations in λ was done when running at the operating point

- $N = 1500rpm$
- $Tq = 150Nm$

Sweeps from $\lambda = 1.1$ to $\lambda = 0.75$ was performed with a step size of 0.05.

3.4 Variations in ignition angle - θ_{ign}

Variations in ignition angle was done when running at the operating point

- $N = 1500rpm$
- $Tq = 150Nm$

The normal ignition angle at the chosen operating point was abandoned in three steps, -5 CAD, -10 CAD and -15 CAD. During the tests lambda was set to a fix value ($\lambda = 1$), and the intake air was set to the value that corresponded to the chosen load.

4

Modeling

This chapter treats all the modeling and theory, it is divided into 5 parts

- Theory
- Pressure model 1 - Analytic model
- Pressure model 2 - Closed system model
- Heat release analysis
- Modeling of the engine out temperature
- Sensitivity analysis of estimated parameters

Since having an accurate cylinder pressure model is of high importance when modeling the engine out temperature, two different pressure models was developed and evaluated. Three different methods to model the heat release is also presented.

4.1 Theory

4.1.1 Thermodynamics

Polytropic process

In this thesis several thermodynamic processes are described by a polytropic process. A polytropic process is a process that follows the relation

$$pV^n = C \tag{4.1}$$

where p is the pressure, V is the volume of the control volume, n is a polytropic exponent and C is a constant. Depending on the value of the polytropic exponent, the relation corresponds to different cases

- $n = 0$: Isobaric process - An isobaric process is a process that occurs during constant pressure
- $n = 1$: Isothermal process - An isothermal process is a process in which the temperature remains constant
- $n \to \infty$: Isochoric process - During an Isochoric process the volume is constant
- $n = \frac{c_p}{c_v}$: Isentropic process - A process occurs without transfer of heat, energy is transferred only as work. The process is also considered to be reversible.

First law of thermodynamics

The first law of thermodynamics is the law saying that energy can never be created or destroyed. In an isolated system, the total amount of energy is constant according to the law of conservation of energy. The law is often expressed as

$$\Delta U = \Delta Q - \Delta W \tag{4.2}$$

which means the internal energy in a system is equal to the total amount of heat supplied to the system minus the energy that is lost as work.

4.1.2 Heat transfer

Heat transfer can occur in three different ways, conduction, convection and radiation. A review of each phenomenon follows.

Conduction

Conduction refers to heat transfer in solid materials. The local heat transfer is often expressed by Fourier's law

$$\dot{Q}_{cond} = -k \cdot A \cdot \frac{dT}{dy} \tag{4.3}$$

where A is the cross-section area and k is the thermal conductivity of the material. Applying the equation on a flat and isentropic wall with a finite thickness, gives a linear relation of the temperature across the wall

$$\dot{Q}_{cond} = Ak\frac{(T_{w,i} - T_{w,o})}{b} \tag{4.4}$$

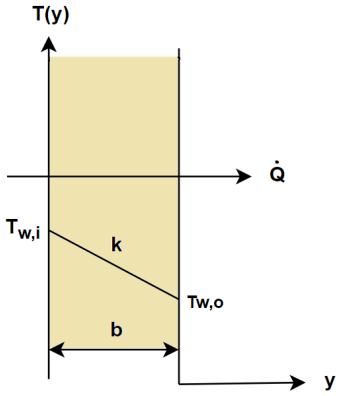

Figure 4.1: *Heat transfer through a wall with thickness b and thermal conductivity k.*

Convection

If heat transfer occurs in a fluid, the heat can only be transferred by conduction if the fluid is standstill. Otherwise, which is the most common case, the heat transfer in a fluid will occur as convection. The movement of the fluid can arise in different ways, by temperature differences in the fluid or when the fluid is forced to move, for example inside the pipes in an engine. The convective heat transfer can be expressed by Newton's law of cooling

$$\dot{Q}_{conv} = A \cdot h(T_1 - T_2) \tag{4.5}$$

where A is the surface area and h is the heat transfer coefficient.

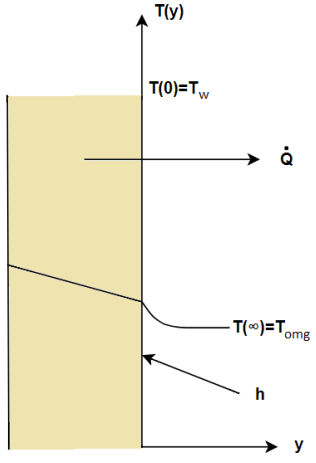

Figure 4.2: *.*

Radiation

Heat transfer by radiation occurs between two surfaces and does not require any carrying intervening medium. Heat transfer by radiation can occur even in vacuum. The maximum heat a body can radiate can be written as

$$\dot{Q}_{rad} = \sigma \epsilon T^4 A \tag{4.6}$$

where T is the temperature $[K]$, A is the surface area of the radiating body and σ is the Stefan-Boltzmann constant which has a value of $5.6703 \cdot 10^{-8}$ $[\frac{W}{m^2 K^4}]$. How efficient a material can emit thermal radiation is described by the emissivity ϵ, which is a function of both surface temperature and radiation wavelength. When describing radiation heat exchange between two bodies, the sum of the two emissivities is used. The expression is

$$\dot{Q}_{rad} = \sigma \epsilon_{12} A (T_1^4 - T_2^4) \tag{4.7}$$

4.1.3 Heat release

When the fuel injected in the cylinder is ignited the fuels chemical energy starts being converted to thermal energy. The behavior of this process can be modeled by doing a heat release analysis. The injected fuel contains of a certain amount of energy. The energy that possibly can be converted to heat can be known by using the lower heating value q_{LHV} [J/kg].

$$Q_{hr} = m_f q_{LHV} \tag{4.8}$$

where m_f is the fuel mass. If the heat release per crank angle is known, the mass fraction burned can be calculated as

$$MFB(\theta) = \frac{\sum_0^\theta dQ_{hr}}{\sum dQ_{hr}} \tag{4.9}$$

4.2 Pressure model 1 - Analytic model

The analytic cylinder pressure model is based on the method described in Eriksson and Andersson [8]. By using the pressure asymptotes for compression and expansion, the pressure trace can be modelled by interpolation between these two asymptotes. Figure 4.4 shows a schematic sketch of the different phases during a cycle.

Input signal(s): p_{ivc}, T_{im}, p_{em}, N, λ, V

Output signals(s): $p(\theta)$, $T(\theta)$

Parameters to estimate: η_f, C_1, C_2,θ_{int}, θ_{exh}, specific heat ratio at compression and expansion, γ_c and γ_e

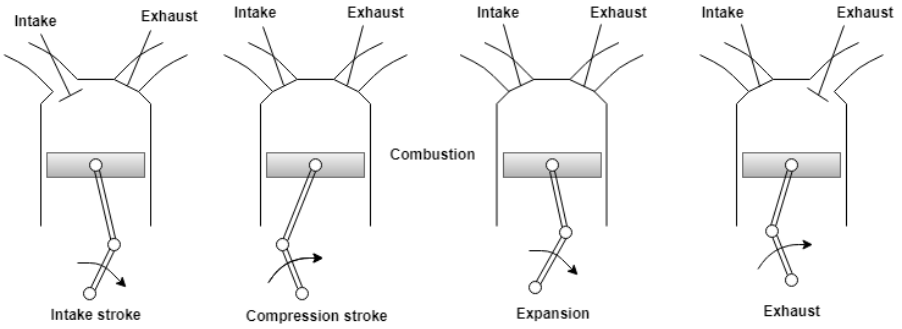

Figure 4.3: *A drawing of the different phases during a cycle.*

4.2.1 Compression

The compression is described by a polytropic process. The polytropic exponent k_c, the reference pressure p_{ivc} and the reference temperature T_{ivc} are used to create models of the pressure and the temperature during compression.

$$p_c(\theta) = p_{ivc}\left(\frac{V_{ivc}}{V(\theta)}\right)^{k_c} \tag{4.10}$$

$$T_c(\theta) = T_{ivc}\left(\frac{V_{ivc}}{V(\theta)}\right)^{k_c-1} \tag{4.11}$$

These two equations will describe the pressure and temperature in the cylinder until the start of combustion.

Initial pressure

The cylinder pressure at the point when the intake valve closes, p_{ivc}, has a great impact on the accuracy of the compression phase model. Therefore it is of great importance to get a good estimation of p_{ivc}. To get the reference pressure, a model based on the intake manifold pressure is used. The pressure can be described by

$$p_{ivc} = p_{im}(\theta_{ivc}) + C_1 + C_2 N \tag{4.12}$$

where N is the engine speed and C_1 and C_2 are tuning parameters. A least square fit was used to fit the parameters, where $p_{im}(\theta_{ivc})$ was used from measured data.

Initial temperature

Since the fluid temperature is influenced by heat transfer and residual gases, it is more difficult to determine the temperature at inlet valve closing compared to the pressure. In this model, the heat transfer is neglected. When fresh air

enters the cylinder the temperature of the air will increase by the hot valves and a locally high heat transfer coefficients, and also by mixing with residual gases. In this model, heat transfer is neglected and therefore the fresh air temperature T_a is approximated to be the same as T_{ivc}. By assuming c_p are the same for the residual gases and fuel mixtures, T_{ivc} can be expressed by

$$T_{ivc} = T_a(1 - x_r) + T_r x_r \tag{4.13}$$

where the residual gas fraction is

$$x_r = \frac{m_r}{m_r + m_f + m_a} \tag{4.14}$$

where T_r is the temperature of the residual gases.
An iterative method to determine x_r and T_r is described in Eriksson and Nielsen [9]. That method has been used by applying following relations

$$x_r = \frac{1}{r_c}\left(\frac{p_{em}}{p_{im}}\right)^{1/\gamma}\left(1 + \frac{q_{in}}{c_v T_1 r_c^{\gamma-1}}\right)^{-1/\gamma} \tag{4.15}$$

$$q_{in} = \frac{1 - x_r}{1 + \lambda(A/F)_s} q_{LHV} \tag{4.16}$$

$$T_r = \left(1 + \frac{q_{in}}{c_v T_1 r_c^{\gamma-1}}\right)^{1/\gamma} \tag{4.17}$$

$$T_1 = x_r T_r + (1 - x_r) T_{im} \tag{4.18}$$

where q_{in} is the specific heat supplied to the system, and T_1 is the cylinder temperature when the intake stroke starts.

The iterative method to determine the residual gas fraction works as follows.

1. Set initial conditions: $x_r = 0$, $T_r = 0$, $q_{in} = 0$ and $T_1 = T_{im}$
2. Find a value of q_{in} by using (4.16)
3. Update the initial values by using (4.15), (4.16), (4.17) and (4.18)
4. Repeat step 3 until the value of x_r and T_r converges, i.e when the change in x_r and T_r is insignificantly small when the process is repeated.

4.2.2 Expansion

Even the expansion phase can be modelled as polytropic process with exponent k_e and by using T_3, p_3 and V_3 as references.

$$p_e(\theta) = p_3\left(\frac{V_3}{V(\theta)}\right)^{k_e} \tag{4.19}$$

$$T_e(\theta) = T_3 \left(\frac{V_3}{V(\theta)} \right)^{k_e - 1} \tag{4.20}$$

T_3, p_3 and V_3 refers to state three in the ideal Otto cycle.
The temperature T_3 can be expressed as the sum of the temperature in phase two and the temperature increase due to the combustion.

$$T_3 = T_2 + \Delta T_{comb} \tag{4.21}$$

Where the temperature increase is determined by

$$\Delta T_{comb} = \frac{m_f q_{LHV} \eta_f(\lambda)}{c_v m_{tot}} \tag{4.22}$$

where $\eta_f(\lambda)$ is the fuel conversion efficiency which is an optimizing parameter. When the temperature T_3 is known the pressure in the same phase can be determined by

$$p_3 = p_2 \frac{T_3}{T_2} \tag{4.23}$$

4.2.3 Combustion

To model the pressure trace during the combustion phase, an interpolation between the compression- and expansion asymptotic pressure traces is done. The interpolation is done by using the Vibe function in Eriksson and Nielsen [9]

$$PR(\theta) = 1 - e^{-a\left(\frac{\theta - \theta_{SOC}}{\Delta\theta} \right)^{m+1}} \tag{4.24}$$

where a and m are parameters which can be expressed as

$$m = \frac{\ln \frac{\ln 1 - 0.1}{\ln 1 - 0.85}}{\ln \Delta\theta_d - \ln (\Delta\theta_d + \Delta\theta_b)} - 1 \tag{4.25}$$

$$a = -\ln (1 - 0.1) \left(\frac{\Delta\theta}{\Delta\theta_d} \right)^{m+1} \tag{4.26}$$

The parameters contains the flame development angle, θ_d, and the rapid burn angle, θ_b. By using these angles, the burn duration can be expressed as

$$\Delta\theta \approx= 2\theta_d + \theta_b \tag{4.27}$$

4.2.4 Valve model

By using a cosine function, the pressure changes when the valves opens and closes can be modelled.

$$x_i(\theta, \theta_0, \theta_1) = 0.5 \left(1 - \cos \left(\pi \frac{\theta - \theta_0}{\theta_1 - \theta_0} \right) \right) \tag{4.28}$$

The model is used during three different phases

- $[\theta_{int} \leq \theta < \theta_{ivc}]$ - When the intake valve start to close until it is completely closed

- $[\theta_{evo} \leq \theta < \theta_{exh}]$ - The blow down phase, when the exhaust valve opens until the pressure in the cylinder is the same as the exhaust manifold pressure

- $[\theta_{ivo} \leq \theta < \theta_{evc}]$ - The overlap period when the intake valve is open until the exhaust valve is closed

4.2.5 Summarizing Analytic Pressure Model

Summarizing the expressions for all phases the full pressure model is

$$p_{cyl} = \begin{cases} p_{im} & , \theta_{evc} \leq \theta < \theta_{int} \\ p_{im}(1 - x_i(\theta, \theta_{int}, \theta_{ivc})) + p_c(\theta)x_i(\theta, \theta_{int}, \theta_{ivc}) & , \theta_{int} \leq \theta < \theta_{ivc} \\ p_c(\theta) & , \theta_{ivc} \leq \theta < \theta_{ign} \\ p_c(\theta)(1 - x_b(\theta)) + p_e(\theta)x_b(\theta) & , \theta_{ign} \leq \theta < \theta_{evo} \\ p_e(1 - x_i(\theta, \theta_{evo}, \theta_{exh})) + p_{em}(\theta)x_i(\theta, \theta_{evo}, \theta_{exh}) & , \theta_{evo} \leq \theta < \theta_{exh} \\ p_{em} & , \theta_{exh} \leq \theta < \theta_{ivo} \\ p_{em}(1 - x_i(\theta, \theta_{ivo}, \theta_{evc})) + p_{em}(\theta)x_i(\theta, \theta_{ivo}, \theta_{evc}) & , \theta_{ivo} \leq \theta < \theta_{evc} \end{cases}$$

4.3 Pressure model 2 - Closed system model

This method is based on a single zone model, which treats the cylinder contents as a single gas with homogeneous pressure, temperature, and composition. The model is looking into the energy balance in the cylinder during the phase when both valves are closed. In this model the crevice effects are neglected, based on the assumption that the mass transfer is zero (no leakage). The supplied fuel energy can then be divided into three different parts, work on the piston (dW), heat released (dQ_{ch}) and heat transfer to the cylinder walls (dQ_{ht}). A schematic sketch of the zone is shown in Figure 4.4. The relation is

$$\frac{dU}{d\theta} = \frac{dQ_{ch}}{d\theta} - \frac{dW}{d\theta} - \frac{dQ_{ht}}{d\theta} \tag{4.29}$$

Where computations has a resolution of two times per crank angle.

Input signal(s): p_{im}, p_{em}, N, T_q, λ, V, dQ_{ch}

Output signals(s): $p(\theta)$, $T(\theta)$

Parameters to estimate: c_v, η_f, θ_{exh}

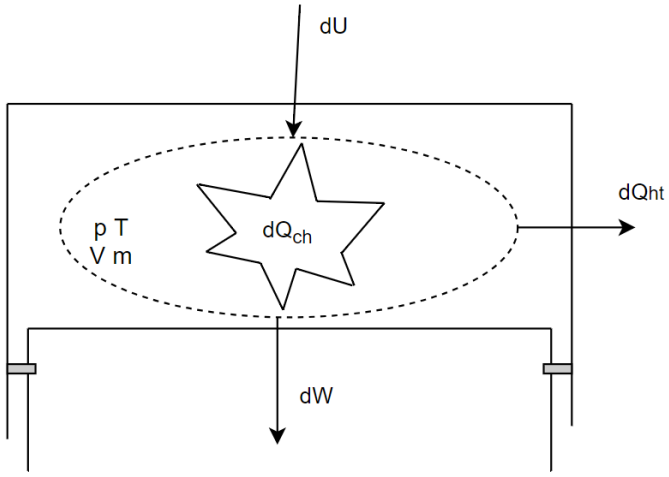

Figure 4.4: *A drawing of the energy balance in the cylinder.*

The internal energy, dU, is derived as the sum of the total mass transferred into the cylinder and the enthalpy of the fuel.

$$\frac{dU}{d\theta} = cv\frac{dT}{d\theta}m \tag{4.30}$$

where $\frac{dT}{d\theta}$ can be calculated using the ideal gas law

$$\frac{dT}{d\theta} = \frac{p\frac{dV}{d\theta} + V\frac{dp}{d\theta}}{mR} \tag{4.31}$$

The work on the piston is calculated by

$$\frac{dW}{d\theta} = \frac{dp}{d\theta}\frac{dV}{d\theta} \tag{4.32}$$

When investigating the heat transfer to the cylinder walls, it is found in Eriksson and Nielsen [9] that the major heat transfer is caused by forced convection. Therefore, the radiation from the gas the cylinder walls is neglected. The heat transfer to the cylinder walls is described by the Newton's law of cooling

$$\frac{dQ_{ht}}{d\theta} = hA\Delta T = hA(T - T_w) \tag{4.33}$$

where A is the area of the cylinder walls and h is the convection heat transfer coefficient. T is the cylinder temperature and T_w is the temperature of the cylinder walls, which in this model is estimated as a constant value.
The convection heat transfer coefficient is determined using a method proposed by Woschni [28]. The expression is

$$h = C_0 B^{-0.2} p^{0.8} w^{0.8} T^{-0.53} \tag{4.34}$$

where $C_0 = 1.3 \cdot 10^{-2}$ and w is the characteristic velocity and is modeled by

$$w = C_1 S_p + C_2 \frac{V T_{IVC}}{V_{IVC} p_{IVC}} (p - p_m) \tag{4.35}$$

The expression of the mean piston speed is $S_p = \frac{2aN}{60}$, where a [m] is the crank radius and N [rpm] is the engine speed. p_m is the motored pressure and the parameters C_1 and C_2 is changed during the cycle

	Gas exchange	Compression	Combustion and expansion
C_1	6.18	2.28	2.28
C_2	0	0	0.00324

To get the heat release, dQ_{ch}, any of the methods in 4.4 is used.
When combining equations 4.29-4.33 the pressure change per crank angle can be expressed as

$$dp = R \frac{dQ_{ch} - Ah_c(T - T_w) - pdV(1 + \frac{c_v}{R})}{c_v V} \tag{4.36}$$

Where c_v is modeled as in Eriksson and Sivertsson [10]. By modeling the initial pressure as $p_{IVC} = p_{im}$, the pressure trace between IVC and EVO can then be iterated by

$$p(i+1) = p(i) + dp(i) \tag{4.37}$$

Using the ideal gas law the temperature during the whole combustion phase is described by

$$T(\theta) = \frac{T_{IVC} p(\theta) V(\theta)}{p_{IVC} V_{IVC}} \tag{4.38}$$

To model the cylinder pressure after EVO, the same cosine function as in (4.28) was used.

4.4 Heat Release analysis

Two different heat release analysis were made, the Rassweiler and Withrow method [9] and a method based on the first law of thermodynamics, which in this thesis is called Closed system method. A third way to determine the heat release is to use the Vibe-function, which is also derived in this chapter.

4.4.1 Rassweiler and Withrow

The Rasswelier-Withrow method does not directly rely to the first law of thermodynamics. As in the closed system method, the input in this method is a pressure trace where the crank angle at each sample is known. The actual pressure

change during combustion can be expressed contributions from two terms, pressure change due to volume change Δp_v and pressure change due to combustion Δp_c.

$$\Delta p = \Delta p_v + \Delta p_c \tag{4.39}$$

The volume change Δp_v is calculated by assuming the pressure change is made up by a polytropic process. The pressure change in every crank angle $\Delta\theta$ is

$$\Delta p_v(j) = p_{j+1,v} - p_j = p_j\left(\left(\frac{V_j}{V_{j+1}}\right)^n - 1\right) \tag{4.40}$$

where n is the polytropic exponent. The pressure change due to combustion can then be expressed as the difference between the actual pressure p_{j+1} and p_v

$$\Delta p_c(j) = p_{j+1} - p_j\left(\frac{V_j}{V_{j+1}}\right)^n \tag{4.41}$$

which is shown in Figure 5.5.

By assuming the pressure change due to combustion is proportional to the fuel that burns, the mass fraction burned can be expressed by

$$MFB_{rw}(j) = \frac{m_b(j)}{m_{b,tot}} = \frac{\sum_{k=0}^{i} \Delta p_c(k)}{\sum_{k=0}^{M} \Delta p_c(k)} \tag{4.42}$$

where M is the total number of samples.

4.4.2 Closed system method

This model is based on the same method as in 4.3. But in this case the pressure trace is considered to be known, and instead, dQ_{ch} is solved from the energy balance.

$$\frac{dQ_{ch}}{d\theta} = \frac{dW}{d\theta} + \frac{dU}{d\theta} + \frac{dQ_{ht}}{d\theta} \tag{4.43}$$

Using the derivations in 4.3, the heat release is

$$\frac{dQ_{ch}}{d\theta} = \frac{dp}{d\theta}\frac{dV}{d\theta} + cv\frac{p\frac{dV}{d\theta} + V\frac{dp}{d\theta}}{mR}m + hA(T - T_w) \tag{4.44}$$

Then, the mass fraction burned is expressed by

$$MFB(i) = \frac{\sum_0^i dQ_{ch}}{\sum_0^M dQ_{ch}} \tag{4.45}$$

4.4.3 Vibe

Even if the Vibe-function is not based on physics, it can approximately be converted to a heat release trace by using its differentiated form

$$\frac{dx_b}{d\theta} = \frac{a(m+1)}{\Delta\theta}\left(\frac{\theta-\theta_0}{\Delta\theta}\right)^m e^{-a\left(\frac{\theta-\theta_{SOC}}{\Delta\theta}\right)^{m+1}} \tag{4.46}$$

By using (4.46), the heat release can be written

$$\frac{dQ_{ch}}{d\theta} = m_f q_{LHV}\eta_f \frac{dx_b}{d\theta} \tag{4.47}$$

where m_f is the fuel injected in kilograms, q_{LHV} is the heat of combustion in J/kg and η_f is the combustion efficiency.

4.5 Modeling of the engine out temperature

When opening the exhaust valve, the gas flow out from the cylinder to the exhaust manifold starts. The temperature change in the cylinder during the blowdown phase can be modeled as an isentropic expansion.

4.5.1 Blowdown phase, $\theta \in [\theta_{EVO}, \theta_{EXH}]$

$$T(\theta) = T_{EVO}\left(\frac{p_{cyl}(\theta)}{p_{EVO}}\right)^{1-1/\gamma} \tag{4.48}$$

The mass in the cylinder and the mass flow flow per crank angle is

$$m(\theta) = \frac{p_{cyl}(\theta)V(\theta)}{RT(\theta)} \tag{4.49}$$

$$\dot{m}_e(\theta_i) = \frac{m(\theta_{i-1}) - m(\theta_i)}{\theta_i - \theta_{i-1}} \tag{4.50}$$

4.5.2 After blow-down, $\theta \in [\theta_{EXH}, \theta_{IVO}]$

After the blow-down, the remaining mass in the cylinder is

$$m_{abl} = \frac{p_{cyl}(\theta_{EXH})V(\theta_{EXH})}{RT(\theta_{EXH})} \tag{4.51}$$

And the temperature of the remaining gas

$$T_{abl} = T(\theta_{EXH}) \tag{4.52}$$

After the blow-down, the cylinder pressure is assumed to be equal to the exhaust manifold pressure, p_{em}. Therefore, the remaining gas minus the residual gases is assumed to flow out at constant pressure and temperature due to (4.52) where the residual gases is

$$m_r = m_{tot} \cdot x_r \tag{4.53}$$

4.5.3 Out temperature

By summing up all the mass that flows out from the cylinder, a mean value exhaust temperature can be expressed according to Ainouz and Vedholm [1]

$$T_{ev} = \frac{\int_{\theta_{EVO}}^{\theta_{EXH}} \dot{m}_e(\theta)T(\theta)d\theta + (m_{abl} - m_r)T_{abl}}{m_{tot} - m_r} \tag{4.54}$$

4.6 Sensitivity analysis of estimated parameters

4.6.1 Cylinder pressure at intake valve closing - p_{ivc}

The cylinder pressure at IVC is estimated as $p_{im,ivc}$. To get an idea of how sensitive the model is for bad estimated values, a sensitivity analysis was done. In Figure 4.5 the blue plot shows the engine out temperature T_{ev} for different p_{ivc}. The red plot shows the corresponding deviation in p_{ivc} in percent, against the change in T_{ev} in percent. It can be seen that a lower estimated value of the intake pressure causes a larger deviation i T_{ev}, than it does for a to high estimated value.

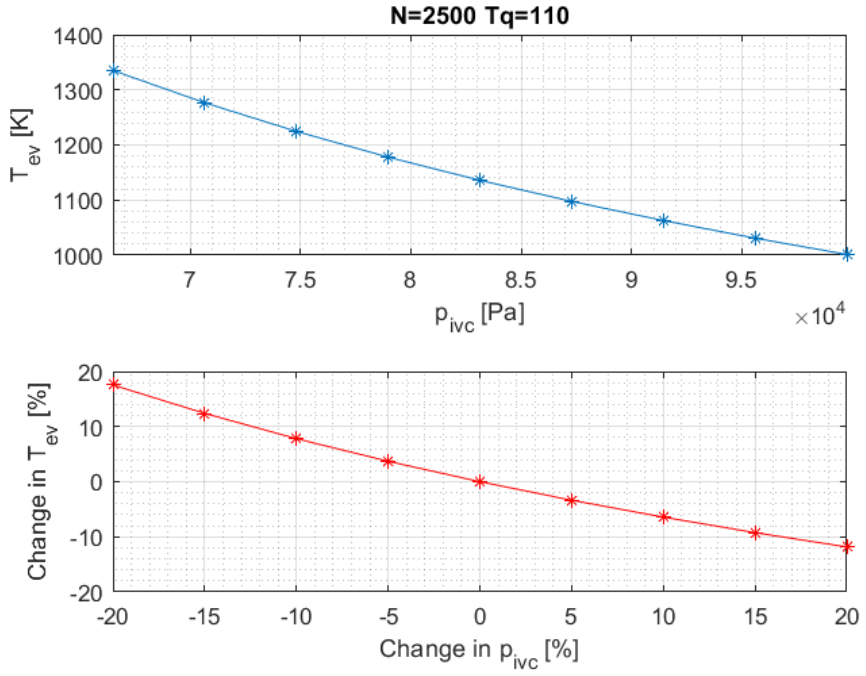

Figure 4.5: *Sensitivity analysis of the temperature model - considering different p_{ivc}.*

Table 4.1: *The sensitivity analysis in Figure 4.5 in tabular form.*

Variations in p_{ivc}	**Change in T_{ev}**
+20%	-11.8%
+15%	-9.2%
+10%	-6.4%
+5%	-3.4%
0	0
-5%	3.7%
-10%	7.8%
-15%	12.4%
-20%	17.6%

4.6.2 Cylinder intake temperature - T_{ivc}

The temperature at IVC can be hard to estimate because it depends on the amount of residual gases. In Figure 4.6 the engine out temperature is compared against different T_{ivc}. As can be seen the out temperature is increasing with higher intake temperatures. The temperature change is also more linear than it is when the intake pressure is changed.

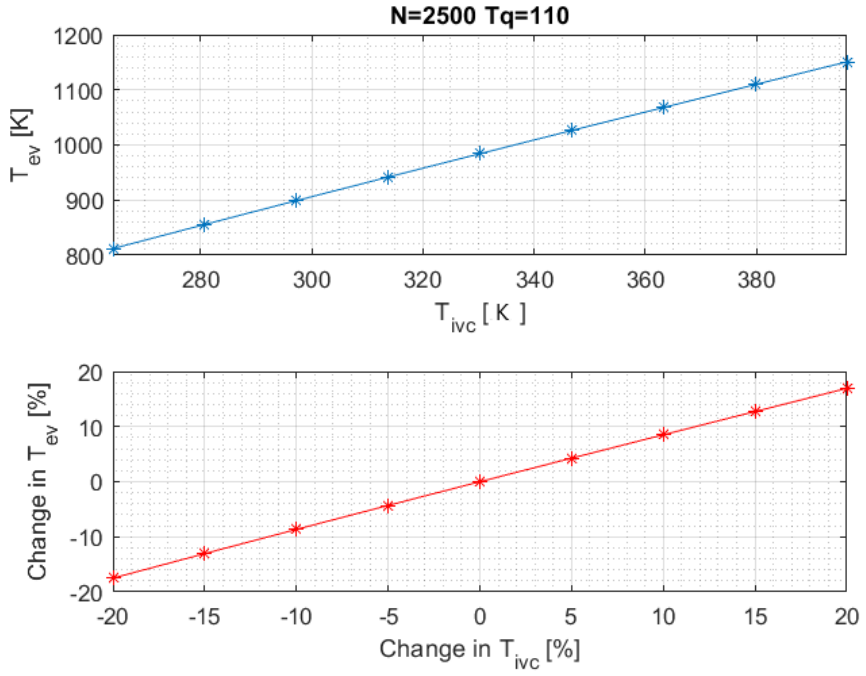

Figure 4.6: *Sensitivity analysis of the temperature model - considering different* p_{ivc}

Table 4.2: *The sensitivity analysis in Figure 4.6 in tabular form.*

Variations in T_{ivc}	**Change in** T_{ev}
+20%	+16.9%
+15%	+12.7%
+10%	+8.5%
+5%	+4.3%
0	0
-5%	-4.3%
-10%	-8.7%
-15%	-13.1%
-20%	-17.5%

5
Results

This chapter is divided into four parts. The first section will cover the pressure models, the second the heat release analysis, the third the temperature sensors and the fourth the engine out temperature.

5.1 Cylinder Pressure Model Validation

5.1.1 Validation of Pressure Model 1 - Analytic pressure model

The analytic pressure model is in this section validated against measured data. The model validation is in this chapter presented by comparing with measured cylinder pressure in three different operating points, one low speed-low load, one medium speed-medium load and high speed-high load. The operating points are

- N=1500 rpm, Tq=65 Nm
- N=2500 rpm, Tq=110 Nm
- N=4000 rpm, Tq=300 Nm

For more operating points, see Appendix A.
In Figure 5.1, 5.2 and 5.3 the modeled pressure is validated for each operating point. The plots in Figure 5.1a, 5.2a and 5.3a shows the compression and expansion asymptotes together with the modeled and measured pressure, which makes the interpolation between the two asymptotes more understandable. In the plots in Figure 5.1b, 5.2b and 5.3b only the modeled and measured pressure are plotted. These figures shows the full cycle pressure.

For each of the three operating points the model is able to match the measured pressure with good accuracy. At higher loads the model error is increasing

around EVO but decreasing over the whole cycle. The operating point with best accuracy between IVC and EVO is N=1500 rpm, Tq=65 Nm but over the whole cycle this point has larger mean relative error than the operating point with highest speed and highest load. Table 5.1 shows the mean relative error for each operating point.

Table 5.1: *Mean relative errors between the analytic pressure model and the measured pressure.*

Operating point	Mean relative error (-360 ° to 360 °)	Mean relative error (IVC to EVO)	Mean relative error (EVO to EXH)
1500 rpm, 65Nm	5.4%	2.3%	1.6%
2500 rpm, 110Nm	4.2%	2.4%	3.1%
4000 rpm, 300Nm	9.1%	1.4%	8.9%

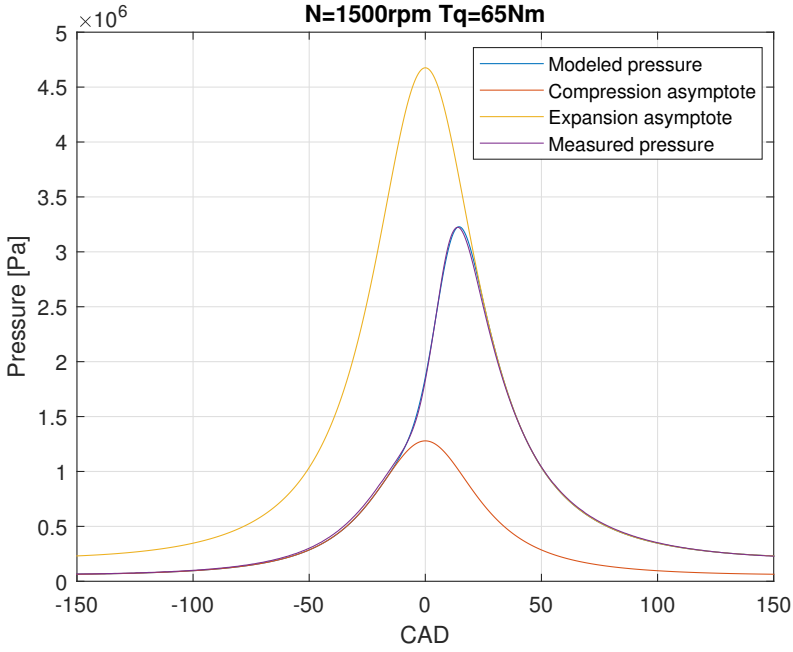

(a) *Compression and expansion asymptotes together with the modeled and measured pressure.*

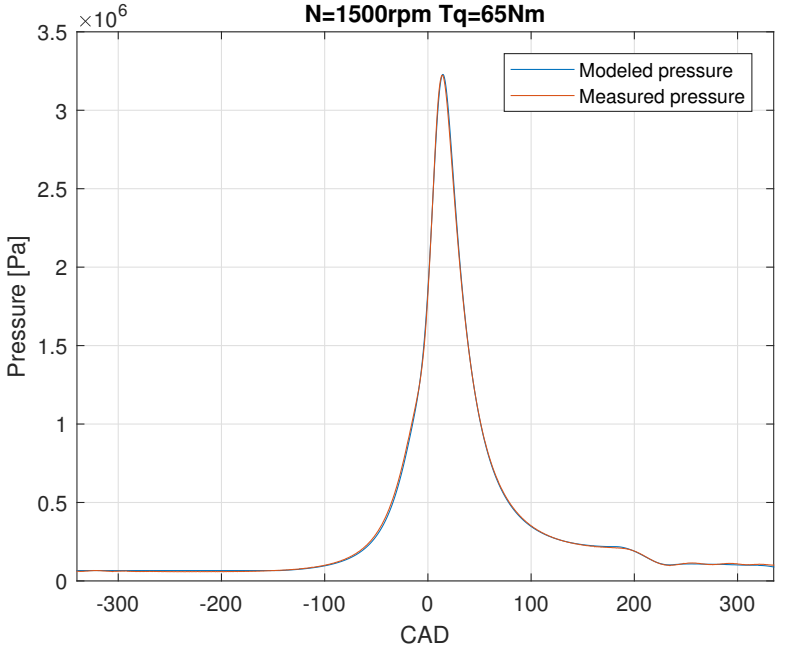

(b) *The modeled and measured pressure trace over the full cycle.*

Figure 5.1: *Cylinder pressure at engine speed $N = 1500rpm$ and load $m_a = 0.44\ g/rev$. The mean relative error from IVC to EVO is 2.3% and over the whole cycle 5.3%.*

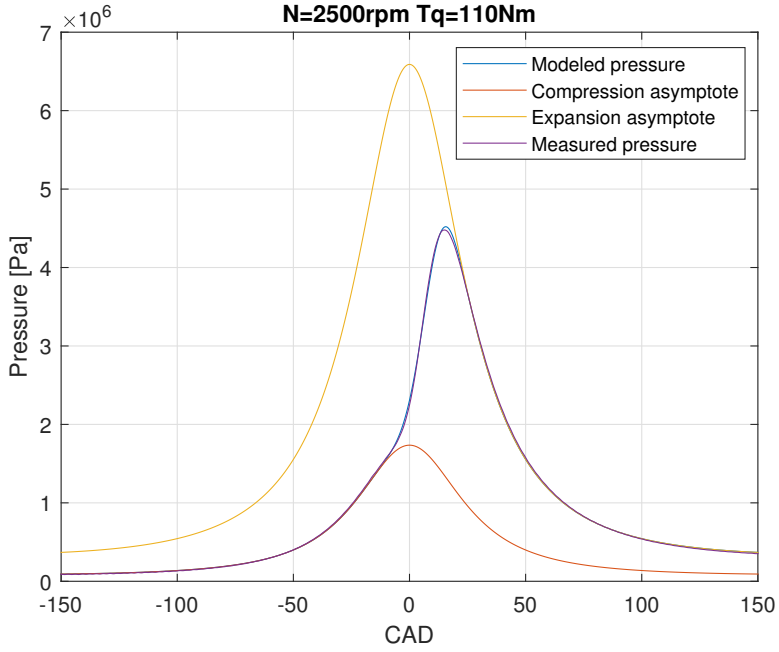

(a) *Compression and expansion asymptotes together with the modeled and measured pressure.*

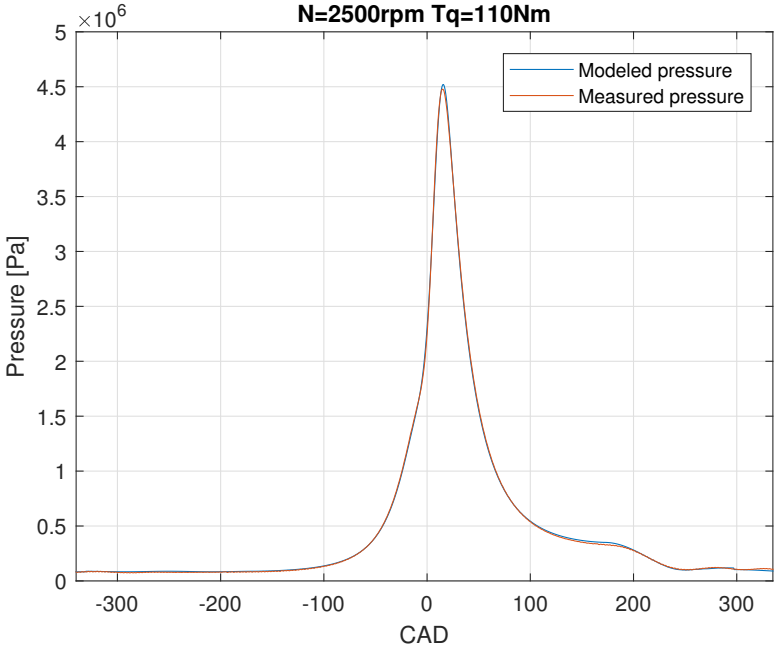

(b) *The modeled and measured pressure trace over the full cycle.*

Figure 5.2: *Cylinder pressure at engine speed $N = 2500rpm$ and load $m_a = 0.68\ g/rev$. The mean relative error from IVC to EVO is 2.4% and over the whole cycle 4.2%.*

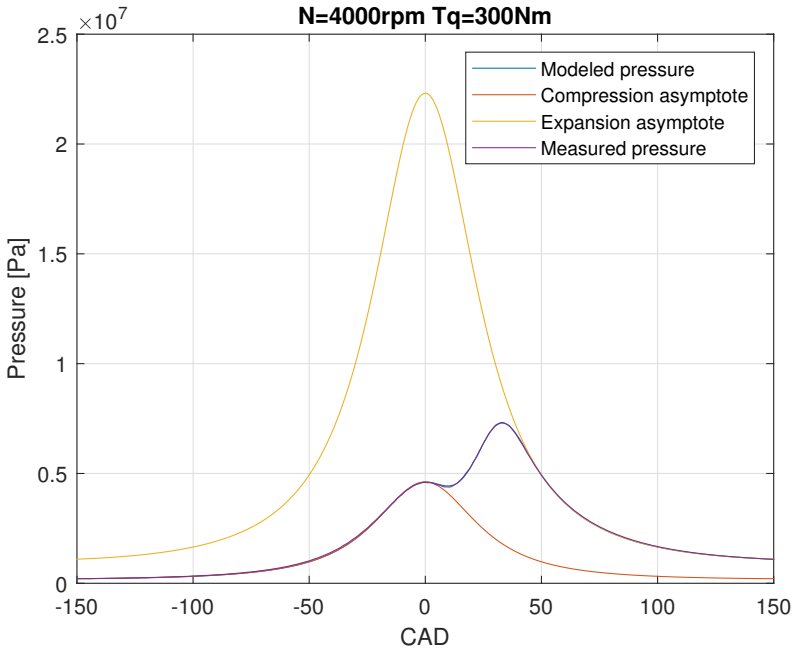

(a) *Compression and expansion asymptotes together with the modeled and measured pressure.*

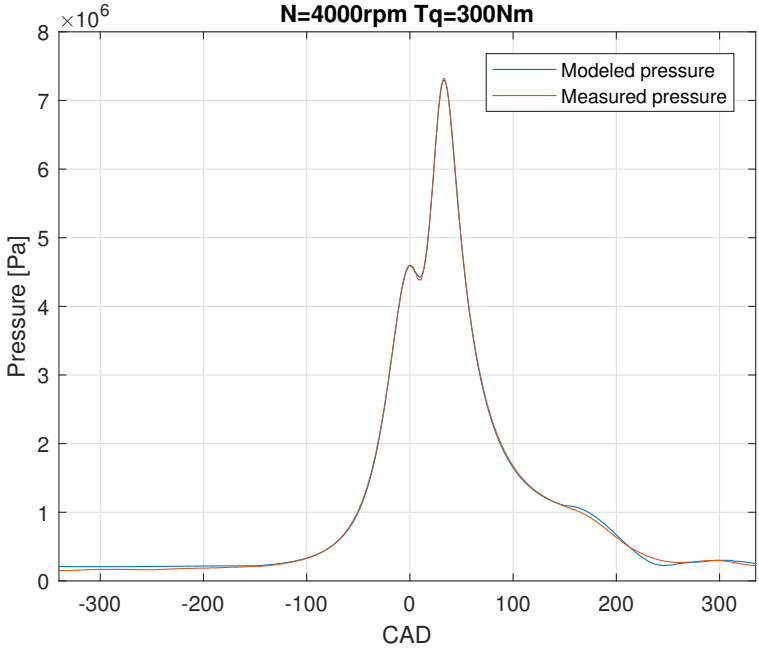

(b) *The modeled and measured pressure trace over the full cycle.*

Figure 5.3: *Cylinder pressure at engine speed 4000rpm and load* $m_a = 1.95\ g/rev$. *The mean relative error from IVC to EVO is 1.4% and over the whole cycle 9.1%.*

5.1.2 Validation of Pressure model 2 - Closed system pressure model

Heat release traces from each of the analysis methods in 4.4 was tested with the closed system pressure model. Since the heat releases from the closed system heat release analysis method was most compatible with the pressure model, this method was used in the validation. The model is validated by using the same engine operating points as for the analytic model validation. Mean relative errors has been calculated for the full cycle, the section between IVC and EVO and between EVO and EXH. For more operating points, see Appendix A.

A measured pressure trace was used to create the heat release as described in chapter 4.4. The heat release is then used as input in the pressure model, which is then validated against the measured pressure. The model is able to follow the measured pressure with good accuracy, see 5.4. A minor noisy behaviour appears around TDC for all operating points. At higher loads, the model is a bit off around θ_{ign}, and the deviation between EVO and EXH is bigger as well.

Table 5.2: *Mean relative errors between the Closed system pressure model and the measured pressure.*

Operating point	Mean relative error (-360 ° to 360 °)	Mean relative error (IVC to EVO)	Mean relative error (EVO to EXH)
1500 rpm, 65Nm	3.6%	2.7%	5.1%
2500 rpm, 110Nm	3.7%	2.9%	4.5%
4000 rpm, 300Nm	8.5%	2%	8.1%

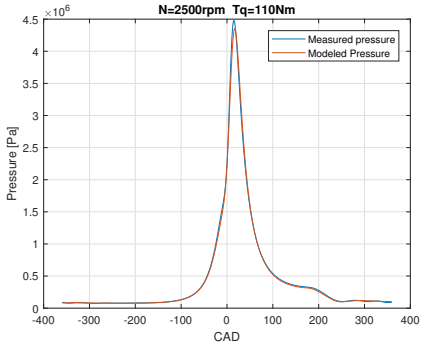

(a) The modeled pressure against the measured pressure. The mean relative error is 3.7%.

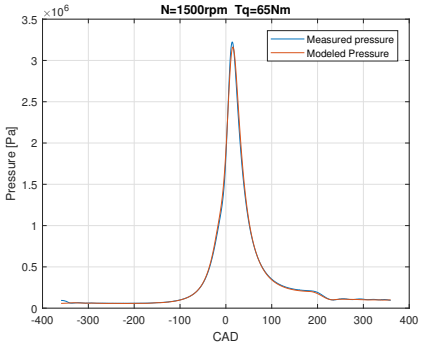

(b) The modeled pressure against the measured pressure. The mean relative error is 3.6%.

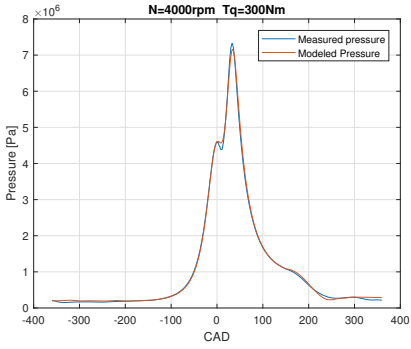

(c) The modeled pressure against the measured pressure. The mean relative error is 8.5%.

Figure 5.4: *Measured pressure against modeled pressure when a heat release from the closed system method is used.*

5.2 Heat release

The different heat releases has been compared to each other and used as input in the closed system pressure model. It turned out that the closed system heat release method was most compatible with the pressure model. Some plots of the different method follows.

Rassweiler/Withrow

In Figure 5.5 it can be seen how the different pressure traces is related to each other. The red line, Δp_c is then used to calculate the mass fraction burned.

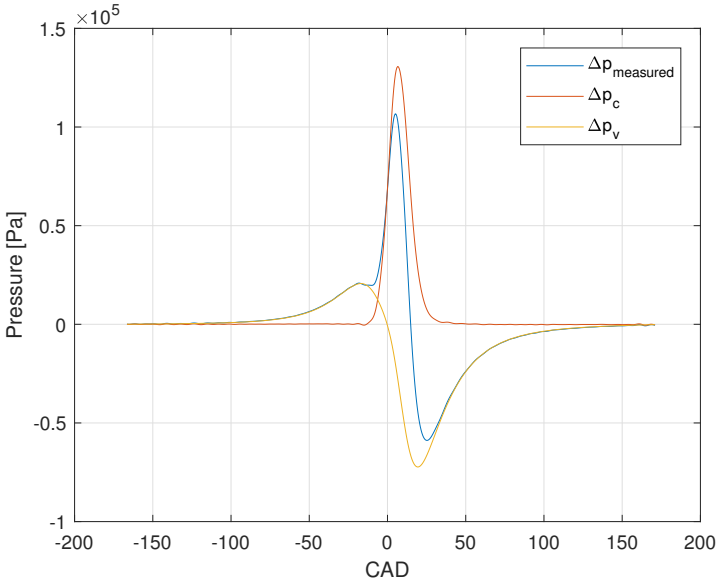

Figure 5.5: *The actual pressure change, the pressure change due to combustion and the pressure change due to volume change.*

Closed system method

In Figure 5.6 it can be seen how the fuel energy is distributed during combustion. The dQ_{ch}-trace is then used to calculate a mass fraction burned.

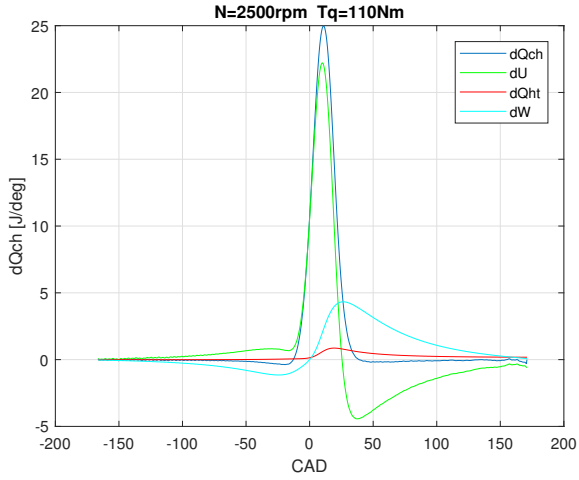

Figure 5.6: *The powers during combustion.*

Vibe

The Vibe-function can approximately be seen as a mass fraction burned trace, even if it is not based on any physical assumptions. Figure 5.7 shows a plot of mass fraction burned traces from each of the heat release analysis methods.

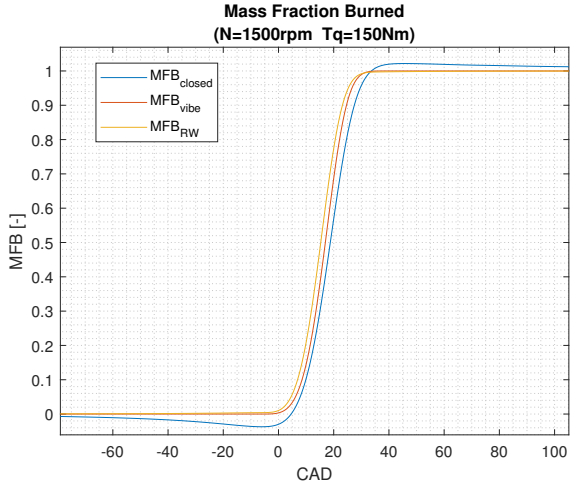

Figure 5.7: *Mass fraction burned from all three methods. The Vibe and Rassweiler/Withrow-traces raises earlier than the MFB from the closed system. The closed system MFB dips before start rising, which indicates the heat transfer to the cylinder walls could be a bit miscalculated.*

5.3 Temperature sensors

The three different temperature sensor differs a lot in their performances, as expected. In Figure 5.8 the behaviour of the exposed thermocouple is plotted against the unexposed thermocouple. The unexposed thermocouple can not catch the pulsations as the exposed thermocouple, since it having a protecting mantle which isolate the thermocouple. In Figure 5.9, the characteristics of the exposed thermocouple and the fine wire thermocouple is shown. The plot shows the temperature during a long sweep with different steps in ignition angle, which explains the periodical ups and downs in temperature. As can be seen the fine wire thermocouple is way faster than the unexposed thermocouple, and could therefore catch the gas pulsations out from the cylinder in a better way.
It is also notably that the fine wire thermocouple show small pulsations after the blow down, which is probably caused by the pressure raise during the blown down from the other cylinders.

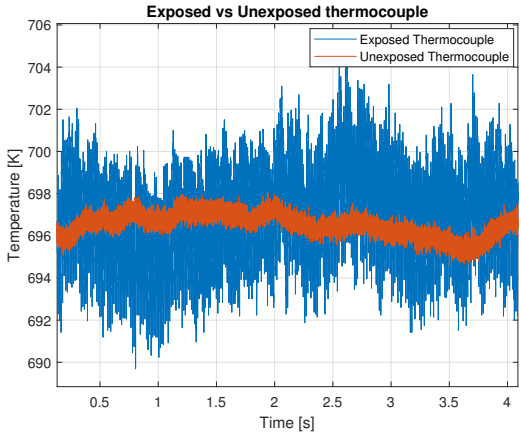

(a) *Exposed thermocouple vs unexposed thermocouple.*

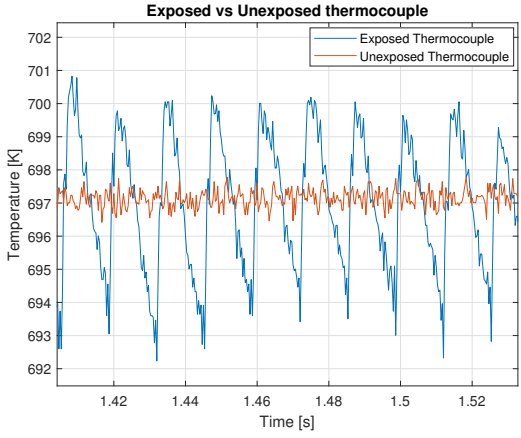

(b) *Zoomed version of 5.8a*

Figure 5.8: *Comparision between an exposed thermocouple and an unexposed thermocouple. The unexposed thermocouple does not catch the pulsations from the exhaust port openings.*

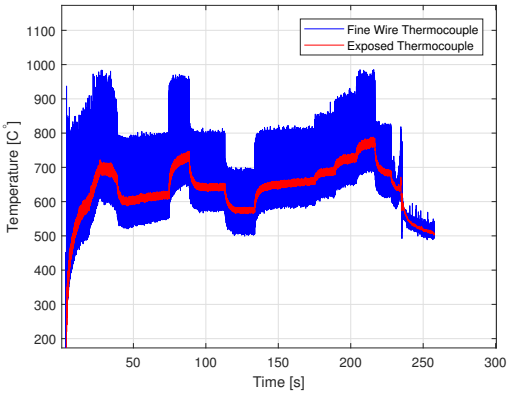

(a) Exhaust port temperature during different steps in ignition angle.

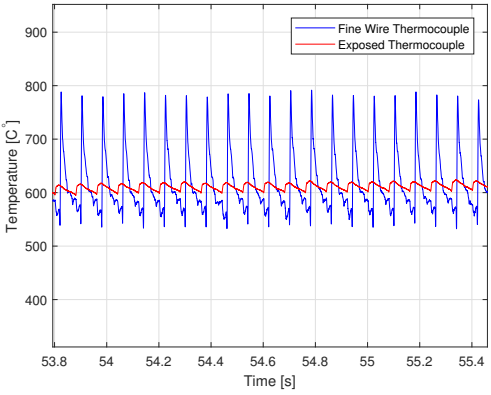

(b) Zoomed figure that show the pulsations.

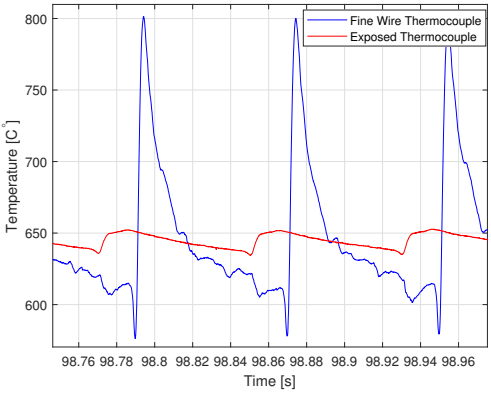

(c) Inzoomed pulsation.

Figure 5.9: *The temperature measured by a fine wire thermocouple and a exposed thermocouple. The fine wire thermocouple is way faster than the exposed thermocouple. It catch higher temperature peaks during blow down but also lower dips between the blow downs. The sensors are placed at different cylinder ports, which explain why the temperature traces are phase shifted.*

5.4 Engine out temperature

The measured temperatures are presented in three different cases.

- Varying loads
- Varying lambda
- Varying ignition angles

In the temperature plots the pipe temperature, port temperature and the engine out temperature are compared.

5.4.1 Varying loads

The operating points described in chapter 3 has been used to validate the engine out temperature model. The two pressure models and a measured pressure trace are all used to validate the temperature model. In Figures 5.10, 5.11 and 5.12 the modeled engine out temperature for each cylinder pressure is shown together with the measured port temperature and the measured pipe temperature.

Measured pressure

The engine out temperature produced with the measured pressure is marked with blue in the current figures. These curves can be seen as the most accurate values since the measured pressure is used. As can be seen the pipe temperature sensors shows a higher temperature than the port temperature sensors. The expected error between modeled engine out temperature and the measured port temperature seem to be quite constant for all loads.

Using analytic pressure model

The engine out temperature produced with the measured pressure is marked with red in the current figures. It can be seen that the difference between measured port temperature and the temperature model are higher than it is when using the measured pressure. At high loads, the model corresponds better to the measured pressure model.

Using closed system pressure model

The yellow curves in the current figures represents the engine out temperature produced with the closed system pressure model. As can be seen the modeled temperature is very low for low loads and low speeds, compared to the other engine out temperatures. The modeled temperature is in the operating point (N=3000rpm,Tq=50) lower than the pipe temperature, which is not reasonable. The model is corresponding better to the measured pressure model at high loads.

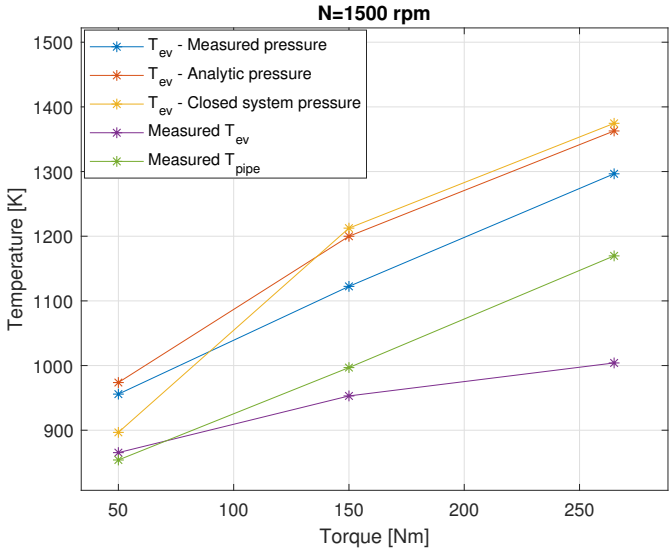

Figure 5.10: *The modeled and measured temperature at 1500 rpm and different loads.*

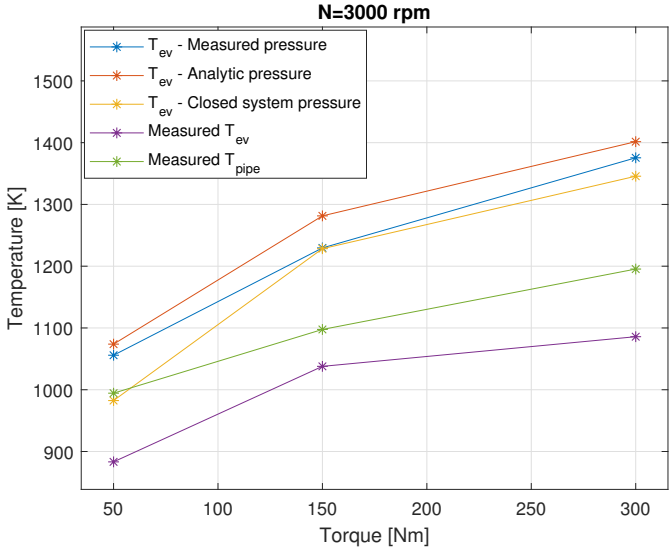

Figure 5.11: *The modeled and measured temperature at 3000 rpm and different loads. The modeled exhaust valve temperature based on the closed system pressure model is at 50 Nm lower than the pipe temperature. That indicates that the closed system pressure model is not accurate in that point.*

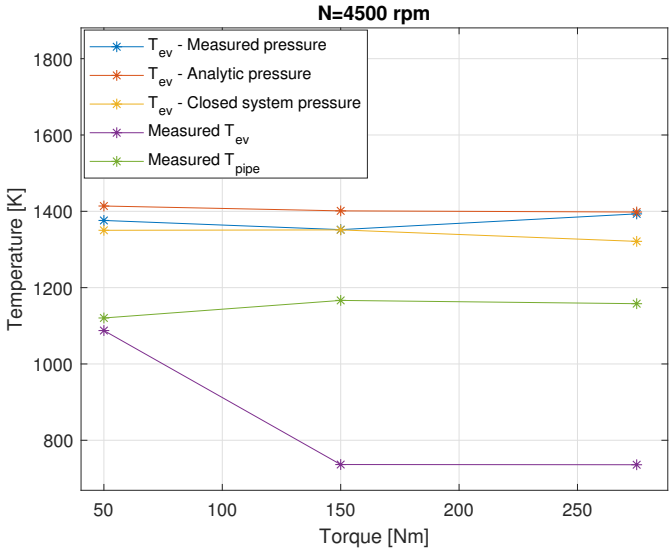

Figure 5.12: *The modeled and measured temperature at 4500 rpm and different loads. It can be seen that the engine is fuel enriching at the two highest loads, witch causes the temperature drop in these points.*

5.4.2 Varying lambda

The lambda values described in Chapter 3 has been used to validate the engine out temperature model. In Figure 5.13 the different temperatures are shown. The port temperature does not show a consistent behaviour through the lambda sweep, like the pipe temperature does. It shows a temperature peak at $\lambda = 1$ and then the temperatures is decreasing by decreasing lambda values. For $\lambda > 1$ the temperature is decreasing as well. The models shows the same tendency but not as distinct as the pipe temperature.

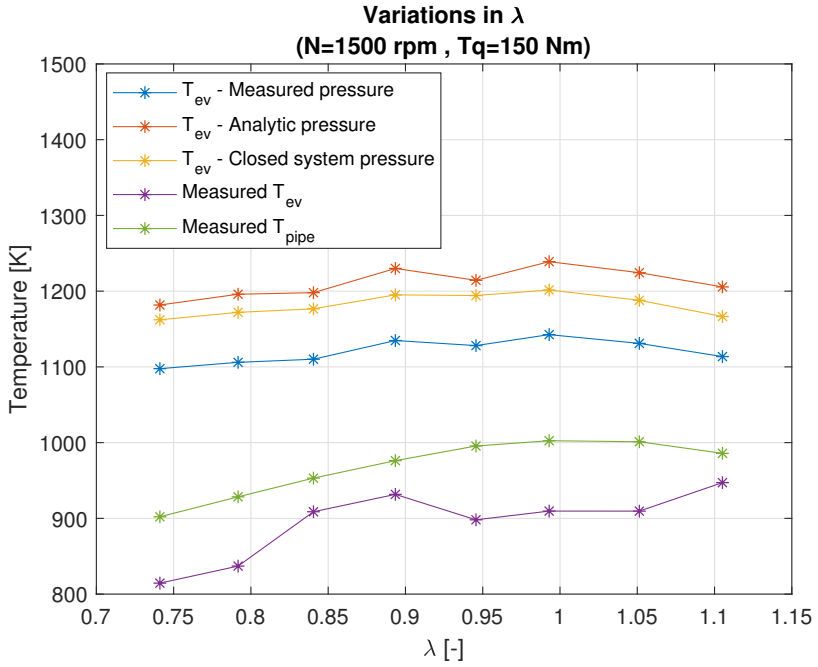

Figure 5.13: *Measured and modeled temperatures for different lambda values.*

5.4.3 Varying ignition angle

In Figure 5.14 the ignition angles in Chapter 3 is used to validate the engine out temperature model. The plot shows that the pipe temperature is consistently increasing when the ignition angle is postponed, so do the model as well. The measured engine out temperature does not have the same consistently appearance. How the cylinder pressure changes for all ignition angles can be seen in Figure 5.15.
Note that when changing the ignition angle with fixed λ and θ_{ign} the load will change. Therefore, the operating points will not be consistent during the ignition angle sweep.

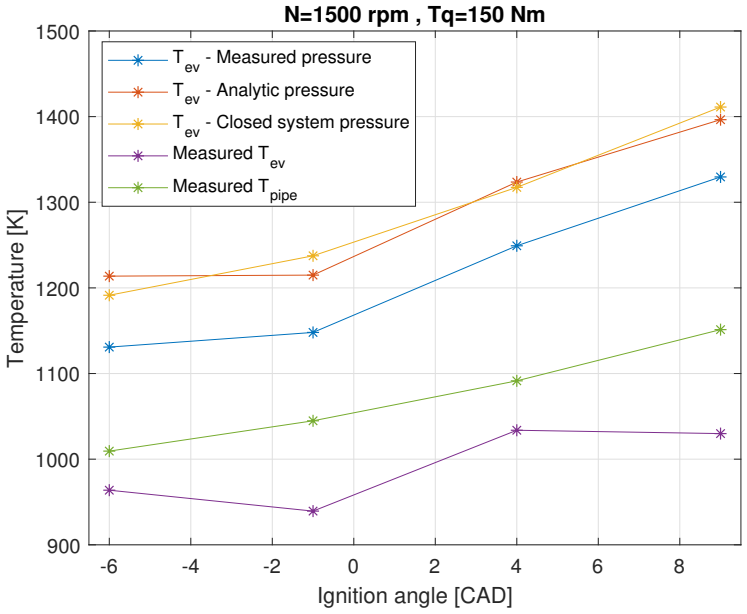

Figure 5.14: *Measured and modeled temperatures for different ignition angles.*

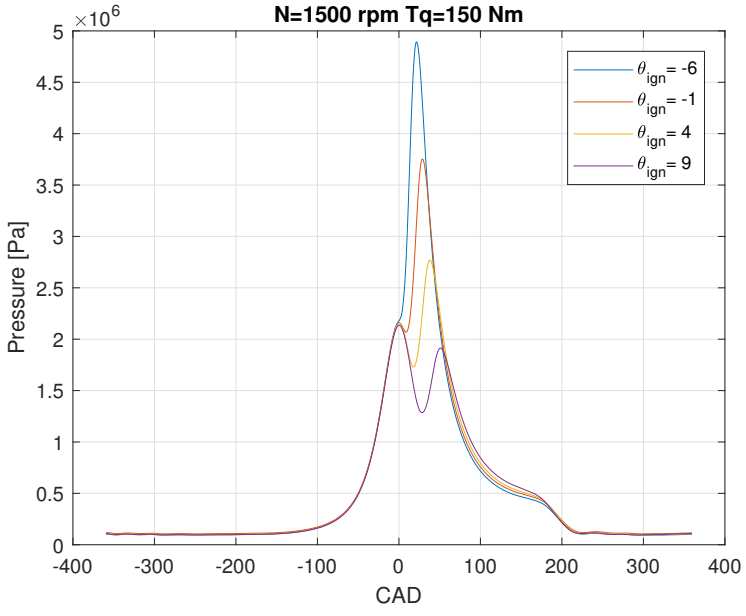

Figure 5.15: *The cylinder pressure for different ignition angles.*

6

Discussion

6.1 Pressure models

The two pressure models show good accuracy when comparing to measured data. Their characteristics are almost equivalent considering mean relative errors, where the biggest deviations occur at high loads.
The compression part of the analytic pressure model that is modeled as a polytropic process has been proved being very accurate for all operating points. The same applies for the expansion asymptote which seem to be able to follow measured data very well. The Vibe function is capable of making the model fit to the measured pressure during combustion with surprisingly good precision. The cosine function that is used during valve openings is able to make the model match the measured pressure during intake valve closing. During exhaust valve opening the model has some problem to follow the measured pressure when running the engine at high loads, where the measured pressure decreases with a steeper inclination than the model. That is a problem since the pressure change during this period is of high importance when modeling the engine out temperature. In this case, the consequences will be a higher engine out modeled temperature due to this model error.
The closed system pressure model is also capable of describe the measured cylinder pressure with good accuracy in all operating points. The model has, just like the analytic model, most difficult to make accurate pressure traces at high loads. An exception applies for the period between IVO and EVO where the model gets more accurate for higher loads, this applies for the analytic pressure model as well. Just like the analytic model this pressure model has hard to follow pressure during the EVO-EXH period at high loads, but is slightly more accurate than the analytic model. Since the main input in the closed system pressure model is a heat release trace, any of the heat release analysis methods should be compatible

with the model. Unfortunately, the model did not manage to create accurate pressure traces when using heat releases created by the Vibe and Rassweiler/Withrow-methods. The pressure has a tendency to raise to too high levels when using these heat releases. At lower loads, there is a major pressure error around TDC and the model still gives accurate pressures at EVO. But at high operating points the pressure gets too high even at EVO, which makes the model useless for the engine out temperature modeling. Therefore, the heat release from the closed system method was used in the pressure model.

6.2 Engine out temperature

The modeled engine out temperature differs depending on which pressure model that is used. Overall, the temperature model gives higher temperatures when using any of the pressure models, comparing to when using measured pressure. When using the analytic pressure model the engine out temperature model usually gives higher temperatures than when using the closed system model.

6.2.1 Varying loads

For all operating points all temperatures increases with increasing loads, which is a reasonable behaviour since more energy is released during the combustion. An unreasonable observation is that the pipe temperature sensors shows higher temperatures than the port temperature sensor does. It should not be possible since there should be a major heat loss in the exhaust pipe. Therefore, when validating the model the pipe temperature sensors are best to use as references. Unfortunately, a model of the heat transfer from exhaust port to temperature sensor was not made due to lack of time. But the model shows a quite acceptable difference between the pipe sensors which indicates that the modeled temperatures are reasonable and a model of the temperature drop from the exhaust port to the pipe sensor should give accurate temperatures. When looking at the engine out temperature plots for the highest loads, it can be seen that the temperature is not increasing anymore. That is because the engine fuel enriches to avoid too high exhaust temperatures.

6.2.2 Varying lambda

When varying λ the pipe temperature peaks at $\lambda = 1$. When fuel enriching ($\lambda < 1$), the temperature will decrease because of several reasons. First by lowering the temperature at IVC due to the higher amount of fuel that is going to evaporate. The temperature will also decrease because of the incomplete combustion, due to the lack of air. It can also be seen that the temperature is decreasing when using too lean mixtures. The reason for that is that the engine is more efficient at leaner mixtures, which means more fuel energy will go to work production. The port temperature shows a more incoherent behavior and it is more difficult to see

a tendency in the temperature change. It can be seen that the models are better in catching lean mixtures than rich mixtures.

6.2.3 Varying ignition angle

When θ_{ign} is moved from $\theta_{ign,opt}$, the temperature is increasing. A delayed ignition timing will reduce the engine efficiency which leads to a higher engine out temperature, so the results are reasonable. The model shows the same tendency which indicates that the model can catch variations in ignition angles. Unfortunately, the same errors remains between the pressure model based temperatures and the measure pressure based temperatures.

6.2.4 Fine wire thermocouples

The fine wire thermocouples have not been used to validate the model but contributed valuable knowledge to the thesis. It was proven that the temperature peaks during blow down are much higher than the exposed thermocouples can show. But they also show lower dips in temperature during the time when the exhaust valve is closed. Therefore, the mean value temperature will not be significant higher when measuring with the fine wire thermocouples. In that sense, these measurements can not explain the strange fact that the port temperature sensors are measuring a lower temperature than the pipe temperature sensor does.

7

Conclusions

The developed model can describe the engine out temperature with promising results. The model is hard to validate since the temperature sensor that is placed near the exhaust port does not show the actual temperature. When validating to the exhaust pipe temperature it was shown that the model is able to follow the direction of the temperature change for different operating points, varying lambda and varying ignition angles. It is hard to establish that the model gives correct absolute level temperature since the model does not consider heat losses in the exhaust port or in the exhaust manifold between the port and the pipe sensor. However, the model has proven to be able to describe temperature changes in pipe temperature even if the temperature differs a lot. In that sense, the model gives reasonable temperatures.

The developed cylinder pressure models corresponds to the measured pressure with good accuracy during almost the whole cycle. During combustion the models correspond to the measured pressure very well but unfortunately the largest deviations were found in the blow down phase, where it is of high importance to know the actual pressure. However, the cylinder pressure models could be used for modeling the engine out temperature with acceptable accuracy.

7.1 Future work

There are several things that can be done to improve the model in the future. Here follows a list of some areas that could be of interest in the future work.

1. Implement a heat transfer model in the exhaust port. A lot of heat is lost in the exhaust port which is significant when modeling the engine out temperature. In Caton and Heywood [2], the authors have developed a model of the heat transfer in an engine exhaust port that can be used.

2. Implement a heat transfer model in the exhaust manifold. As long as the exhaust temperature sensors does not measure the actual temperature, there is need to take the exhaust manifold heat transfer into account. Otherwise, the model can not be validated accurately enough.

3. Improve the cylinder pressure models. The pressure models shows good accuracy during almost the whole cycle, an exception occurs during the blow down phase at high loads. Since it is very important to have an accurate cylinder pressure model in this phase, the engine out model can be improved by improving the pressure model.

4. The model has been validated in 9 operating points which is acceptable. But for securing the characteristics of the model, more data would be preferred. Especially for the variations of lambda and ignition angles, where the sweeps was only made in one single operating point.

5. Make a model of the temperature sensors. To solve the problem with the inaccurate port temperature measuring, it could be a good idea to develop a model of the temperature sensors. If modeling the sensor as a cylindrical shaped body enclosed in a pipe, it could be interesting to calculate all kinds of heat transfer coefficients and see if they are reasonable. This could lead to better understanding of what kind of heat transfer the sensors are actually catching.

Appendix

A

Plots

This appendix consists of cylinder pressure plots for all the tested operating points, as a complement to Chapter 5. Plots of both the analytic cylinder pressure model and the closed system model is shown.

Analytic cylinder pressure model

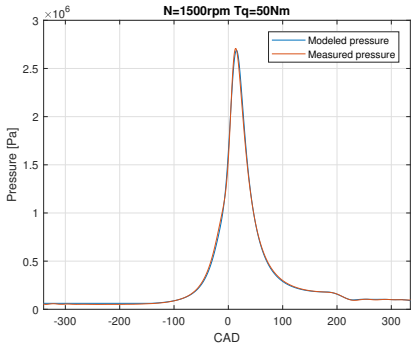

Figure A.1: *Analytic cylinder pressure model*

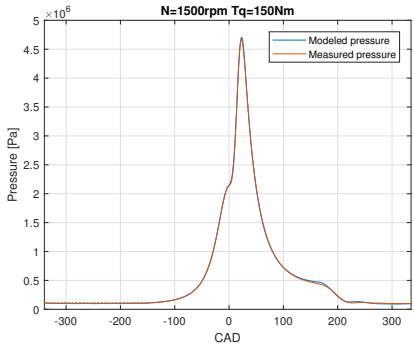

Figure A.2: *Analytic cylinder pressure model*

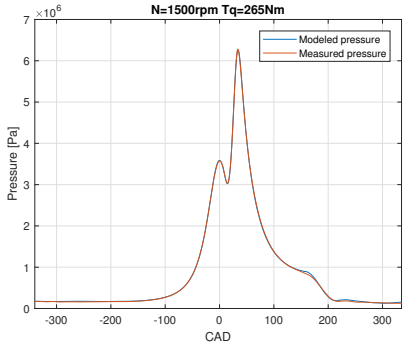

Figure A.3: *Analytic cylinder pressure model*

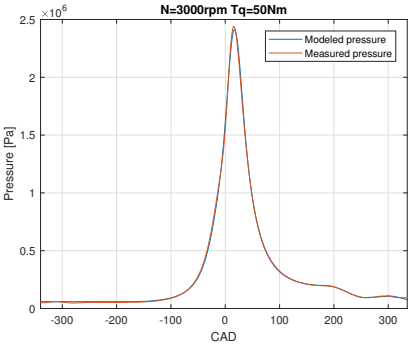

Figure A.4: *Analytic cylinder pressure model*

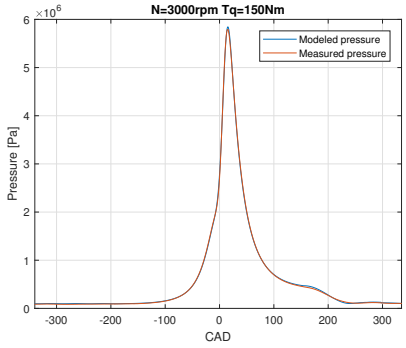

Figure A.5: *Analytic cylinder pressure model*

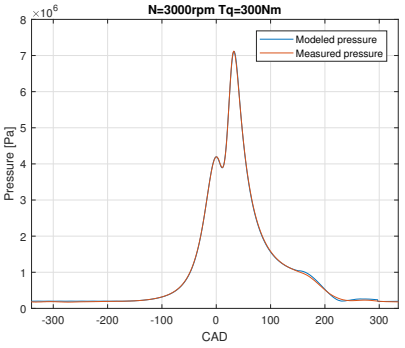

Figure A.6: *Analytic cylinder pressure model*

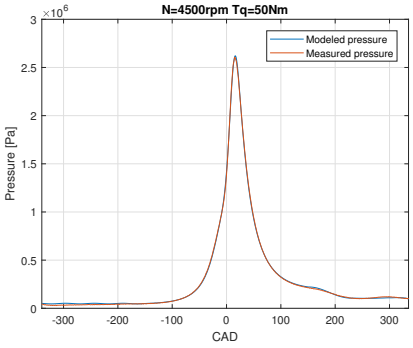

Figure A.7: *Analytic cylinder pressure model*

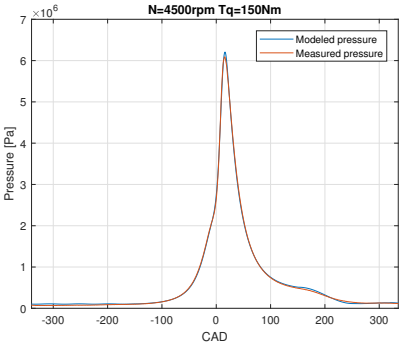

Figure A.8: *Analytic cylinder pressure model*

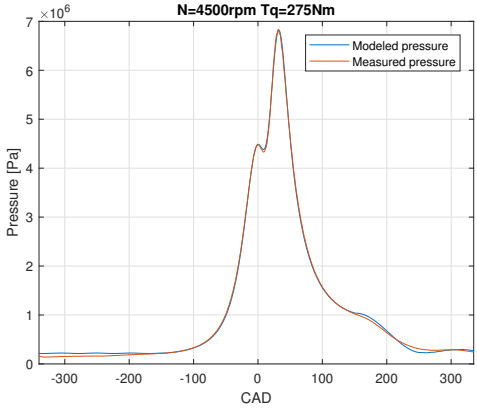

Figure A.9: *Analytic cylinder pressure model*

Closed system cylinder pressure model

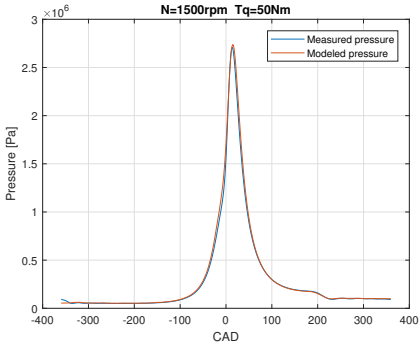

Figure A.10: *Closed system cylinder pressure model*

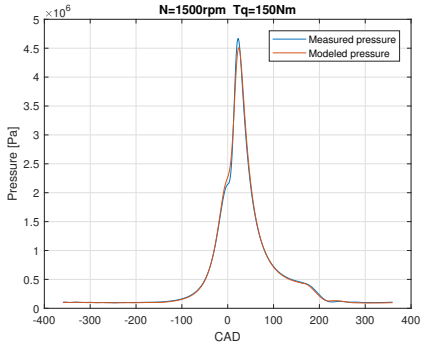

Figure A.11: *Closed system cylinder pressure model*

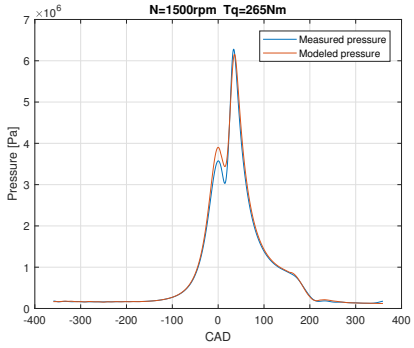

Figure A.12: *Closed system cylinder pressure model*

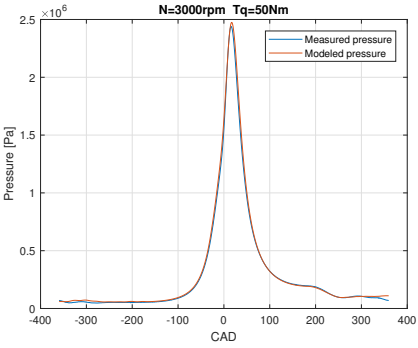

Figure A.13: *Closed system cylinder pressure model*

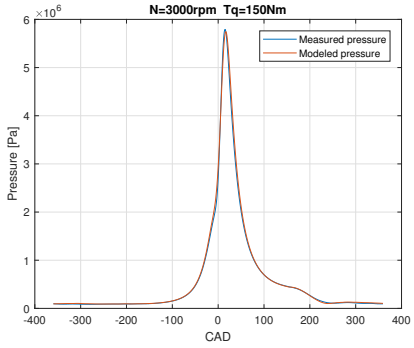

Figure A.14: *Closed system cylinder pressure model*

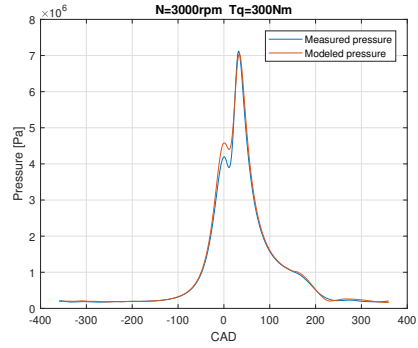

Figure A.15: *Closed system cylinder pressure model*

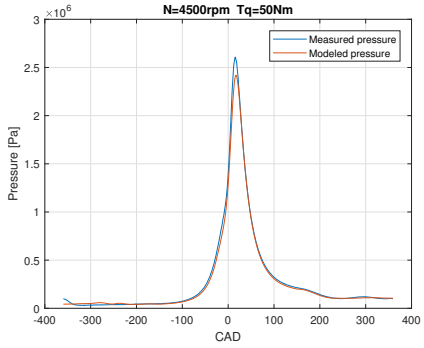

Figure A.16: *Closed system cylinder pressure model*

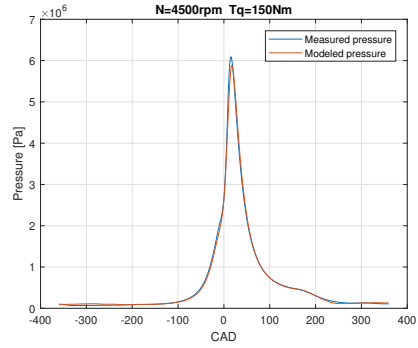

Figure A.17: *Closed system cylinder pressure model*

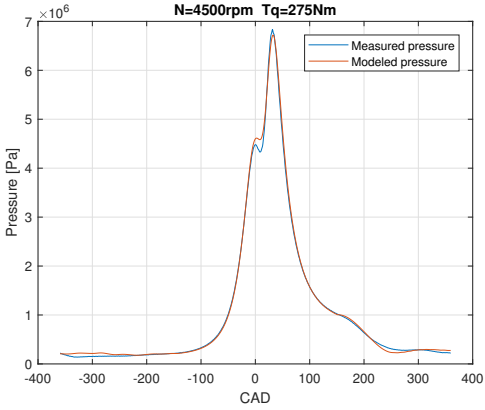

Figure A.18: *Closed system cylinder pressure model*

Bibliography

[1] Filip Ainouz and Jonas Vedholm. Mean value model of the gas temperature at the exhaust valve. Master's thesis, Linköping University, 2009. Cited on pages 5 and 25.

[2] JA Caton and JB Heywood. An experimental and analytical study of heat transfer in an engine exhaust port. *International Journal of Heat and Mass Transfer*, 24(4):581–595, 1981. Cited on page 51.

[3] JA Caton and John B Heywood. Models for heat transfer, mixing and hydrocarbon oxidation in a exhaust port of a spark-ignited engine. *SAE Technical Paper*, (800290), 1980. Cited on page 6.

[4] Nicolò Cavina, Carlo Siviero, and Rosanna Suglia. Residual gas fraction estimation: Application to a gdi engine with variable valve timing and egr. *SAE Technical Paper*, (2004-01-2943), 2004. Cited on page 5.

[5] Charles Stark Draper. The physical effects of detonation in a closed cylindrical chamber. *NASA Technical Report*, 1935. Cited on page 6.

[6] Mikael Ericson, Oskar Graffman, Lars Malm, Martin Blomgren, Haris Subasic, Johan Häggblom, Max Johansson, and Joel Westling. Testplan - förbättrad motoreffektivitet och prestanda med vatteninsprutning. Fordonssystem, ISY, LiU, 2017. URL `http://www.control.isy.liu.se/student/tsrt10/`. Cited on page 6.

[7] Lars Eriksson. Mean value models for exhaust system temperatures. *SAE Technical Paper*, (2002-01-0374), 2002. Cited on page 6.

[8] Lars Eriksson and Ingemar Andersson. An analytic model for cylinder pressure in a four stroke si engine. *SAE Technical Paper*, (2002-01-0371), 2002. Cited on pages 6 and 16.

[9] Lars Eriksson and Lars Nielsen. *Modeling and control of engines and drivelines*. John Wiley & Sons, 2014. Cited on pages 5, 18, 19, 21, and 22.

[10] Lars Eriksson and Martin Sivertsson. Computing optimal heat release rates in combustion engines. *SAE International Journal of Engines*, 8(2015-01-0882):1069–1079, 2015. Cited on page 22.

[11] Jonathan W Fox, Wai K Cheng, and John B Heywood. A model for predicting residual gas fraction in spark-ignition engines. *SAE Technical Paper*, (931025), 1993. Cited on page 5.

[12] Alessandro Franco and Luigi Martorano. Evaluations on the heat transfer in the small two-stroke engines. *SAE Technical Paper*, (980762), 1998. Cited on page 6.

[13] JA Gatowski, En N Balles, KM Chun, FE Nelson, JA Ekchian, and John B Heywood. Heat release analysis of engine pressure data. *SAE Technical paper*, (841359), 1984. Cited on page 6.

[14] Mohit Hashemzadeh Nayeri. Cylinder-by-cylinder torque model of an si-engine for real-time applications. Master's thesis, Linköping University, 2005. Cited on page 6.

[15] Mark J Jennings and Thomas Morel. A computational study of wall temperature effects on engine heat transfer. *SAE Technical Paper*, (910459), 1991. Cited on page 6.

[16] T Leroy, G Alix, J Chauvin, A Duparchy, and F Le Berr. Modeling fresh air charge and residual gas fraction on a dual independent variable valve timing si engine. *SAE International Journal of Engines*, 1(2008-01-0983): 627–635, 2008. Cited on page 5.

[17] Douglas R Martin and Benjamin Rocci. Virtual exhaust gas temperature measurement. *SAE Technical Paper*, (2017-01-1065), 2017. Cited on page 7.

[18] GC Mavropoulos, CD Rakopoulos, and DT Hountalas. Experimental assessment of instantaneous heat transfer in the combustion chamber and exhaust manifold walls of air-cooled direct injection diesel engine. *SAE International Journal of Engines*, 1(2008-01-1326):888–912, 2008. Cited on page 6.

[19] Steve Meisner and SC Sorenson. Computer simulation of intake and exhaust manifold flow and heat transfer. *SAE Technical Paper*, (860242), 1986. Cited on page 5.

[20] Michael Mladek and Christopher H Onder. A model for the estimation of inducted air mass and the residual gas fraction using cylinder pressure measurements. *SAE Technical Paper*, (2000-01-0958), 2000. Cited on page 5.

[21] Per Öberg and Lars Eriksson. Control oriented modeling of the gas exchange process in variable cam timing engines. *SAE Technical Paper*, (2006-01-0660), 2006. Cited on page 5.

[22] F Ponti, JC Piani, and R Suglia. Residual gas model for on-line estimation for inlet and exhaust continuous vvt engine configuration. *IFAC Proceedings Volumes*, 37(22):257–265, 2004. Cited on page 5.

[23] GB Rieker, Hejie Li, Xiang Liu, JTC Liu, JB Jeffries, RK Hanson, MG Allen, SD Wehe, PA Mulhall, HS Kindle, et al. Rapid measurements of temperature and h2o concentration in ic engines with a spark plug-mounted diode laser sensor. *Proceedings of the Combustion Institute*, 31(2):3041–3049, 2007. Cited on page 7.

[24] PK Senecal, J Xin, and Rolf D Reitz. Predictions of residual gas fraction in ic engines. *SAE Technical Paper*, (962052), 1996. Cited on page 5.

[25] PJ Shayler, JP Chick, and T Ma. Correlation of engine heat transfer for heat rejection and warm-up modelling. *SAE Technical Paper*, (971851), 1997. Cited on page 5.

[26] Patrick Michael Smith. *Crevice volume effect on spark ignition engine efficiency*. PhD thesis, Massachusetts Institute of Technology, 2013. Cited on page 6.

[27] Belachew Tesfa, Rakesh Mishra, Fengshou Gu, and AD Ball. Water injection effects on the performance and emission characteristics of a ci engine operating with biodiesel. *Renewable Energy*, 37(1):333–344, 2012. Cited on page 6.

[28] Gerhard Woschni. A universally applicable equation for the instantaneous heat transfer coefficient in the internal combustion engine. *SAE Technical paper*, (670931), 1967. Cited on page 21.